Angewandte Chemie
Eine Zeitschrift der Gesellschaft Deutscher Chemiker

Supporting Information

Chelator-Free Radiolabeling of Nanographene: Breaking the Stereotype of Chelation

*Sixiang Shi, Cheng Xu, Kai Yang, Shreya Goel, Hector F. Valdovinos, Haiming Luo, Emily B. Ehlerding, Christopher G. England, Liang Cheng, Feng Chen, Robert J. Nickles, Zhuang Liu, and Weibo Cai**

anie_201610649_sm_miscellaneous_information.pdf

Supplementary Information

Experimental section

Reagents. ^{64}Cu was produced by a GE PETtrace cyclotron using the ^{64}Ni(p,n)^{64}Cu reaction. ^{89}Zr was produced by a GE PETrace cyclotron using the ^{89}Y(p,n)^{89}Zr reaction. NOTA was purchased from Macrocyclics, Inc. (Dallas, TX). Chelex 100 resin (50-100 mesh; Sigma-Aldrich, St. Louis, MO), complete mouse serum (Jackson Immuno Research Laboratories, West Grove, PA) and PD-10 desalting columns (GE Healthcare, Piscataway, NJ) were all acquired from commercial sources. Water and all buffers were of Millipore grade and pre-treated with Chelex 100 resin to ensure that the aqueous solution was free of heavy metal. All other chemicals and buffers were obtained from Thermo Fisher Scientific (Fair Lawn, NJ).

Cell lines and animal models. 4T1 murine breast cancer cells were obtained from American Type Culture Collection (ATCC, Manassas, VA) and cultured according to the supplier's instructions. When they reached ~80% confluence, the cells were collected for tumor implantation.[1] Four-to-five-week-old female Balb/c mice (Harlan, Indianapolis, IN) were each subcutaneously injected with 2×10^6 4T1 cells in the flank to generate the 4T1 breast cancer model. The mice were used for *in vivo* experiments when the tumor diameter reached 6-8 mm. All animal studies were conducted under a protocol approved by the University of Wisconsin Institutional Animal Care and Use Committee.

Synthesis of RGO-PEG, GO-PEG and derivatives. RGO and GO was produced by a modified Hummers method, using flake expandable graphite as the original material, as detailed in our previous reports.[2] The prepared RGO was mixed with C_{18}PMH-PEG$_{5000}$ at a weight ratio of

1:10 and incubated under sonication for 1.5 h to form RGO-PEG, while the prepared GO was mixed 6-arm PEG (10 kDa) at a weight ratio of 1:6 and reacted for ~12 h in the presence of N-(3-dimethylaminopropyl-N'-ethylcarbodiimide) hydrochloride to form GO-PEG. Excess PEG in the as-synthesized RGO-PEG and GO-PEG solution was removed by centrifugal filtration through 300 kDa MWCO Amicon filters and 100 kDa MWCO Amicon filters and washed with water for 6 times respectively. The resulting RGO-PEG was characterized by atomic-force microscopy and dynamic light scattering. To generate the control nanoconjugates NOTA-PEG-RGO, RGO was firstly modified with C_{18}PMH-PEG$_{5000}$-NH_2 and then reacted with p-SCN-Bn-NOTA at a molar ratio of 1:10 at pH 9.0 for 2 h at room temperature and purified with PD-10 desalting column to yield NOTA-PEG-RGO.[3]

After synthesis of RGO-PEG, NOTA was loaded by incubating with RGO-PEG at a weight ratio of 2:1 for 3 h. The excess NOTA was removed with 100 kDa MWCO Amicon filters. As-prepared NOTA-loaded RGO-PEG was defined as (NOTA)RGO-PEG.

Characterization. The size and morphology of graphene nanosheets were measured by atomic-force microscopy (AFM; Bruker Biospin Corporation, Billerica, MA). The size distribution was further confirmed by dynamic light scattering (DLS) on Nano-Zetasizer (Malvern Instruments Ltd., Worcestershire, UK). Fourier transform infrared (FT-IR) spectra were obtained in the range of 650–3500 cm^{-1} using a Bruker Equinox 55/S FT-IR/NIR Spectrophotometer. Of note, to avoid the inference from PEG, RGO and Cu-RGO nanoparticles for FTIR examination were not PEGylated.

Radiolabeling and labeling stability. $^{64}CuCl_2$ (74 MBq) was diluted in 300 μL of 0.1 M sodium acetate buffer (pH 5.5) and mixed with RGO, GO, RGO-PEG, GO-PEG and their derivatives. The reactions were conducted at 37 ºC for 60 min with constant shaking. The resulting ^{64}Cu-RGO, ^{64}Cu-GO, ^{64}Cu-RGO-PEG, ^{64}Cu-GO-PEG, ^{64}Cu-NOTA-PEG-RGO and (^{64}Cu-NOTA)RGO-PEG were purified by size exclusion column chromatography using PBS as the mobile phase. The labeling yield was measured by thin layer chromatography (TLC) using 0.5 M ethylenediaminetetraacetic acid (EDTA) as the mobile phase to eliminate unstable adsorption of isotopes. The labeling yields at different reaction times were calculated from autoradiography images of TLC plates. To examine the radiolabeling specificity, ^{89}Zr-oxalate (74 MBq) was mixed with RGO-PEG and GO-PEG in 300 μL of 0.5 M HEPES buffer (pH 7.0) at 37 ºC for 60 min with constant shaking. The labeling yields were tested by TLC plates with the same setting as described above.

To test the labeling stability, ^{64}Cu-RGO-PEG, ^{64}Cu-GO-PEG and other controls were incubated in both PBS and complete mouse serum at 37 ºC for up to 24 h under constant shaking. Portions of the mixture were sampled at different time points and filtered through 300 kDa MWCO filter. The radioactivity that remained on the filter was measured after discarding the filtrate, and retained (i.e., intact) ^{64}Cu-RGO-PEG, ^{64}Cu-GO-PEG and their derivatives were calculated using the equation (radioactivity on filter/total sampling radioactivity × 100%).

***In vivo* PET and biodistribution studies.** Serial PET scans of ^{64}Cu-RGO-PEG was performed in 4T1 tumor-bearing mice (n = 6) using a microPET/microCT Inveon rodent model scanner (Siemens Medical Solutions USA, Inc.), at different time points (0.5 h, 3 h, 6 h and 24 h) post-

injection (p.i.) via tail vein. Data acquisition, image reconstruction, and region-of-interest (ROI) analysis of the PET data were performed as previously described.[4] Quantitative data of ROI analysis on tumor and other organs was presented as percentage injected dose per gram of tissue (%ID/g). As control groups, 4T1 mice injected with ^{64}Cu-NOTA-PEG-RGO and (^{64}Cu-NOTA)RGO-PEG were also scanned (n = 3). After the last scan at 24 h p.i., mice were sacrificed under anaesthesia for *ex vivo* biodistribution studies. Tumor, blood and major organs/tissues were collected and weighted. The radioactivity in the tissue was measured using a γ counter (PerkinElmer) and presented as %ID/g (mean ± SD).

Photoacoustic Imaging. Photoacoustic imaging was performed on Vevo LAZR Photoacoustic Imaging System (VisualSonics, Inc., Toronto, Canada) with a laser excitation wavelength of 808 nm and a focal depth of 100 mm. 4T1 tumor-bearing mice were intravenously injected with RGO-PEG (200 μL, 0.2 mg/ml) and scanned at 3 h post-injection. The same volumes of PBS were injected in 4T1 tumor-bearing mice as control groups.

Notes

The authors declare no competing financial interests.

ACKNOWLEDGEMENTS

This work is supported, in part, by the University of Wisconsin–Madison, the National Institutes of Health (NIBIB/NCI 1R01CA169365, 1R01EB021336, P30CA014520, T32CA009206 and T32GM008505), the American Cancer Society (125246-RSG-13-099-01-CCE), and Wisconsin Distinguished Graduate Fellowship. We also gratefully acknowledge the Analytical

Instrumentation Center of the School of Pharmacy at University of Wisconsin–Madison for obtaining FTIR spectra.

Reference:

[1] H. Hong, G. W. Severin, Y. Yang, J. W. Engle, Y. Zhang, T. E. Barnhart, G. Liu, B. R. Leigh, R. J. Nickles, W. Cai, *Eur. J. Nucl. Med. Mol. Imaging* **2012**, *39*, 138-148.

[2] a) K. Yang, S. Zhang, G. Zhang, X. Sun, S. T. Lee, Z. Liu, *Nano Lett.* **2010**, *10*, 3318-3323; b) K. Yang, J. Wan, S. Zhang, B. Tian, Y. Zhang, Z. Liu, *Biomaterials* **2012**, *33*, 2206-2214; c) K. Yang, L. Feng, H. Hong, W. Cai, Z. Liu, *Nat. Protoc.* **2013**, *8*, 2392-2403.

[3] S. Shi, K. Yang, H. Hong, H. F. Valdovinos, T. R. Nayak, Y. Zhang, C. P. Theuer, T. E. Barnhart, Z. Liu, W. Cai, *Biomaterials* **2013**, *34*, 3002-3009.

[4] S. Shi, H. Orbay, Y. Yang, S. A. Graves, T. R. Nayak, H. Hong, R. Hernandez, H. Luo, S. Goel, C. P. Theuer, R. J. Nickles, W. Cai, *J. Nucl. Med.* **2015**, *56*, 927-932.

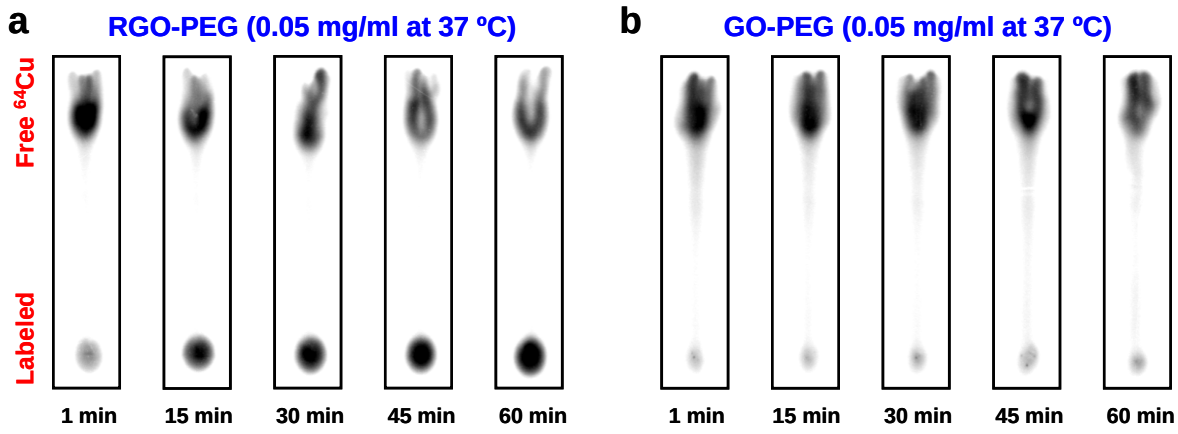

Figure S1. Chelator-free radolabeling of ^{64}Cu on RGO-PEG (**a**) and GO-PEG (**b**) at 0.05 mg/ml at 37 ºC. Autoradiographic images of TLC plates were measured after 1, 15, 30, 45 and 60 min reaction with ^{64}Cu.

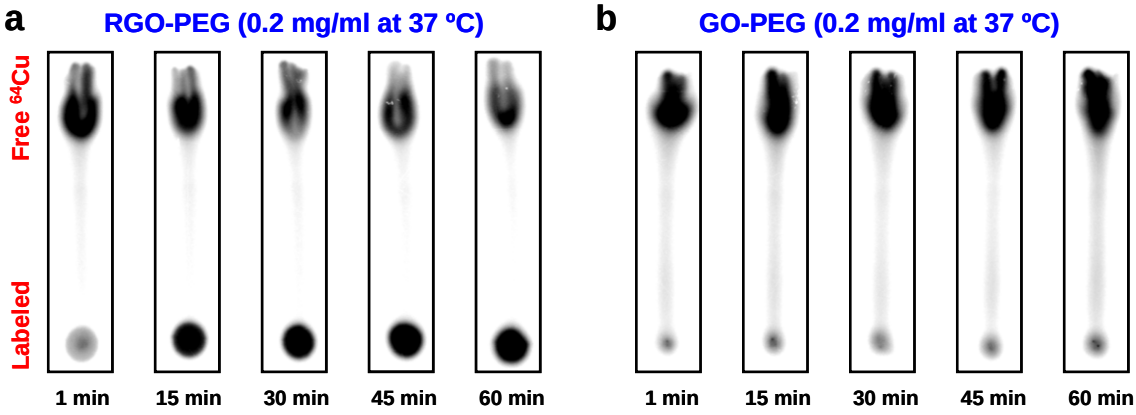

Figure S2. Chelator-free radolabeling of ^{64}Cu on RGO-PEG (**a**) and GO-PEG (**b**) at 0.2 mg/ml at 37 ºC. Autoradiographic images of TLC plates were measured after 1, 15, 30, 45 and 60 min reaction with ^{64}Cu.

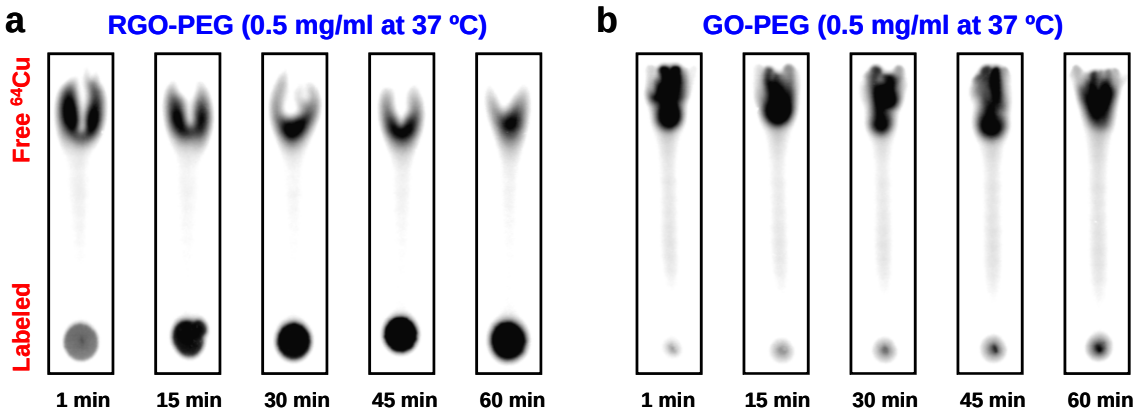

Figure S3. Chelator-free radolabeling of ^{64}Cu on RGO-PEG (**a**) and GO-PEG (**b**) at 0.5 mg/ml at 37 ºC. Autoradiographic images of TLC plates were measured after 1, 15, 30, 45 and 60 min reaction with ^{64}Cu.

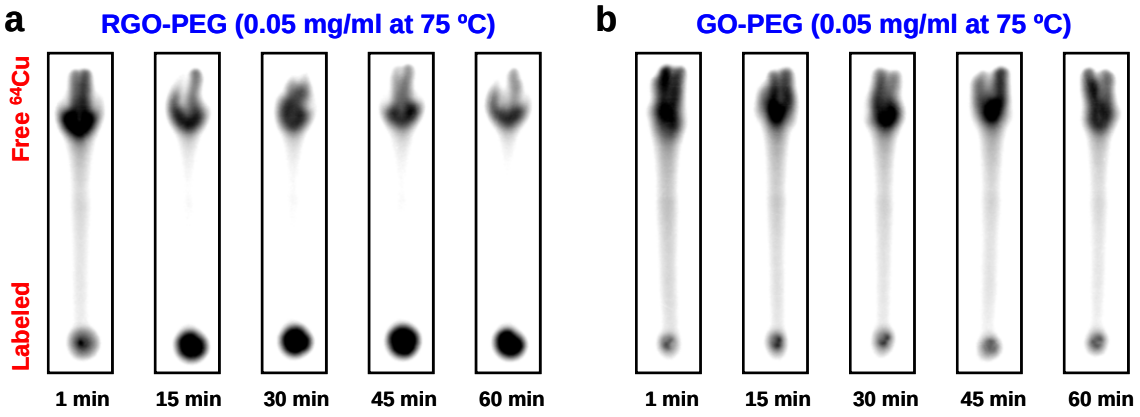

Figure S4. Chelator-free radolabeling of ^{64}Cu on RGO-PEG (**a**) and GO-PEG (**b**) at 0.05 mg/ml at 75 ºC. Autoradiographic images of TLC plates were measured after 1, 15, 30, 45 and 60 min reaction with ^{64}Cu.

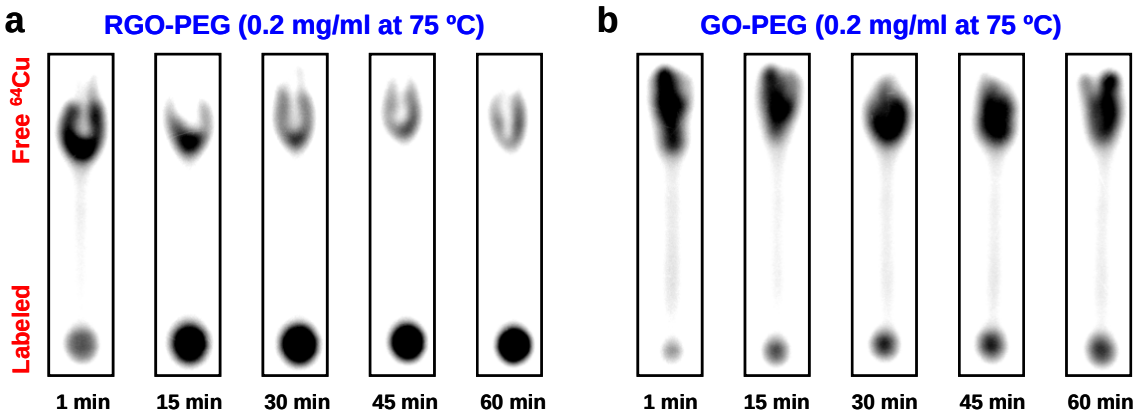

Figure S5. Chelator-free radolabeling of ^{64}Cu on RGO-PEG (**a**) and GO-PEG (**b**) at 0.2 mg/ml at 75 ºC. Autoradiographic images of TLC plates were measured after 1, 15, 30, 45 and 60 min reaction with ^{64}Cu.

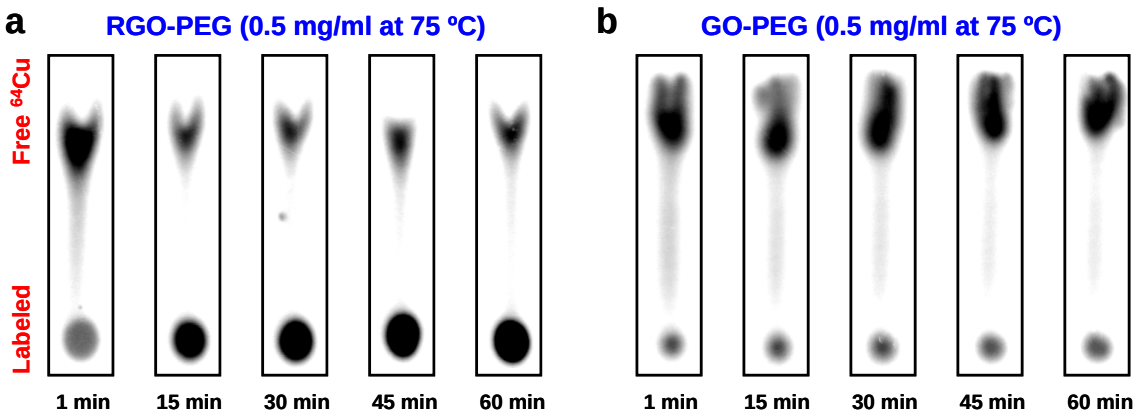

Figure S6. Chelator-free radolabeling of ^{64}Cu on RGO-PEG (**a**) and GO-PEG (**b**) at 0.5 mg/ml at 75 ºC. Autoradiographic images of TLC plates were measured after 1, 15, 30, 45 and 60 min reaction with ^{64}Cu.

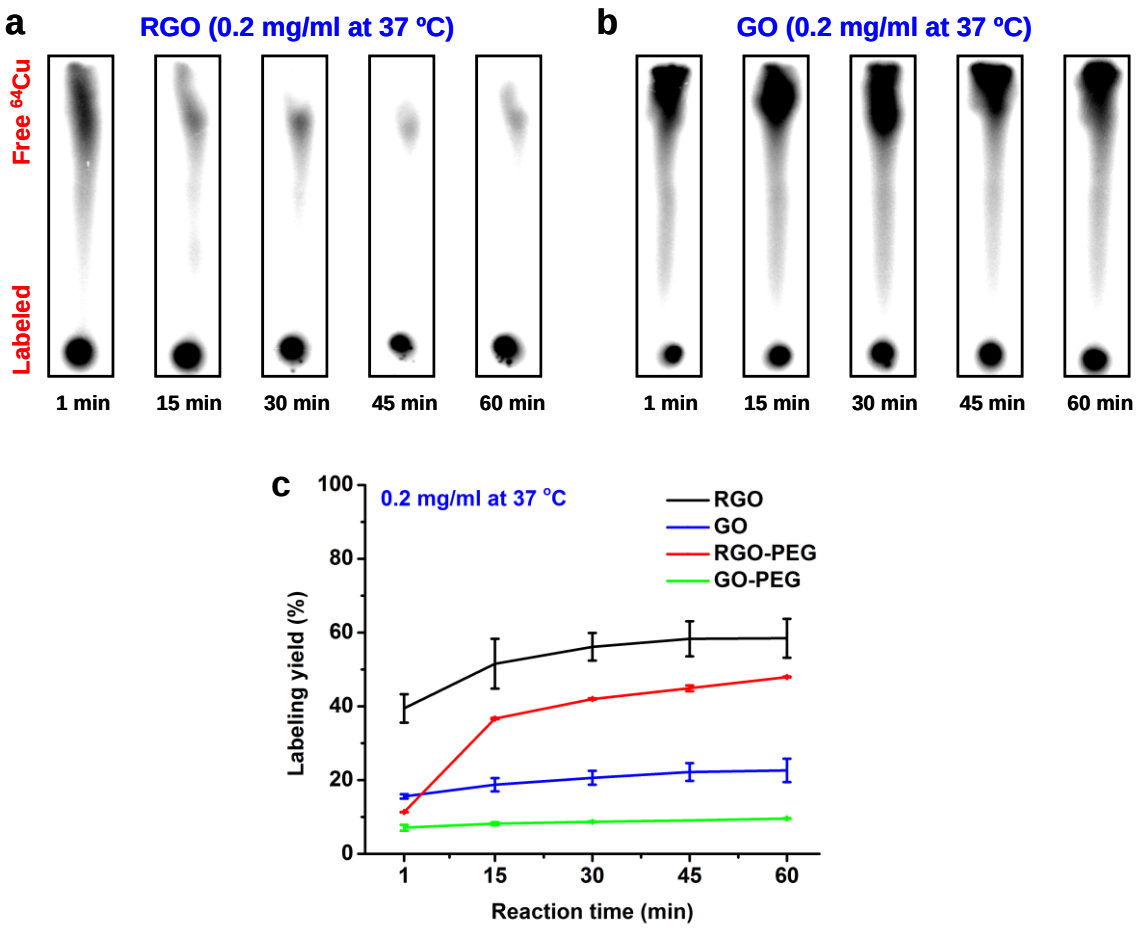

Figure S7. Chelator-free radolabeling of ^{64}Cu on RGO (a) and GO (b) without PEGylation at 0.2 mg/ml at 37 ºC. (c) Autoradiographic images of TLC plates were captured and labeling yields at different time points were acquired after 1, 15, 30, 45 and 60 min reaction with ^{64}Cu, as a comparison with the labeling yields of RGO-PEG and GO-PEG.

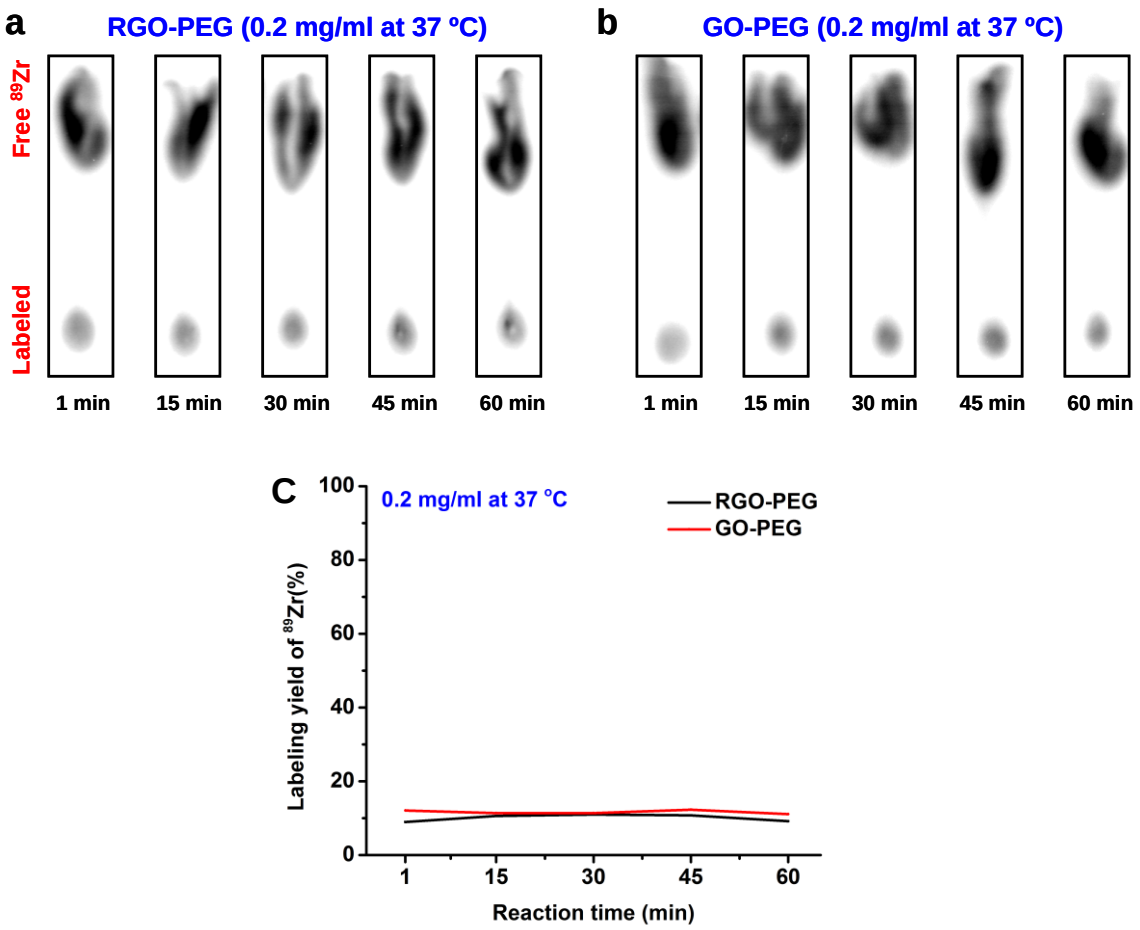

Figure S8. Chelator-free radolabeling of ^{89}Zr on RGO-PEG (**a**) and GO-PEG (**b**) at 0.2 mg/ml at 37 ºC. (**c**) Autoradiographic images of TLC plates were measured and their labeling yields at different time points were acquired after 1, 15, 30, 45 and 60 min reaction with ^{89}Zr.

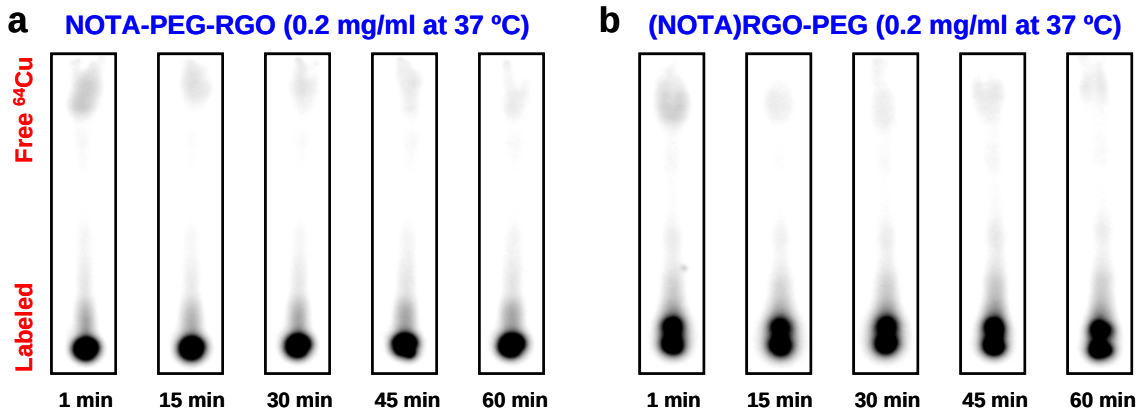

Figure S9. Chelator-free radolabeling of ^{64}Cu on NOTA-conjugated RGO (NOTA-PEG-RGO) (**a**) and NOTA-loaded RGO ((NOTA)RGO-PEG) (**b**) at 0.2 mg/ml at 37 ºC. Autoradiographic images of TLC plates were measured after 1, 15, 30, 45 and 60 min reaction with ^{64}Cu.

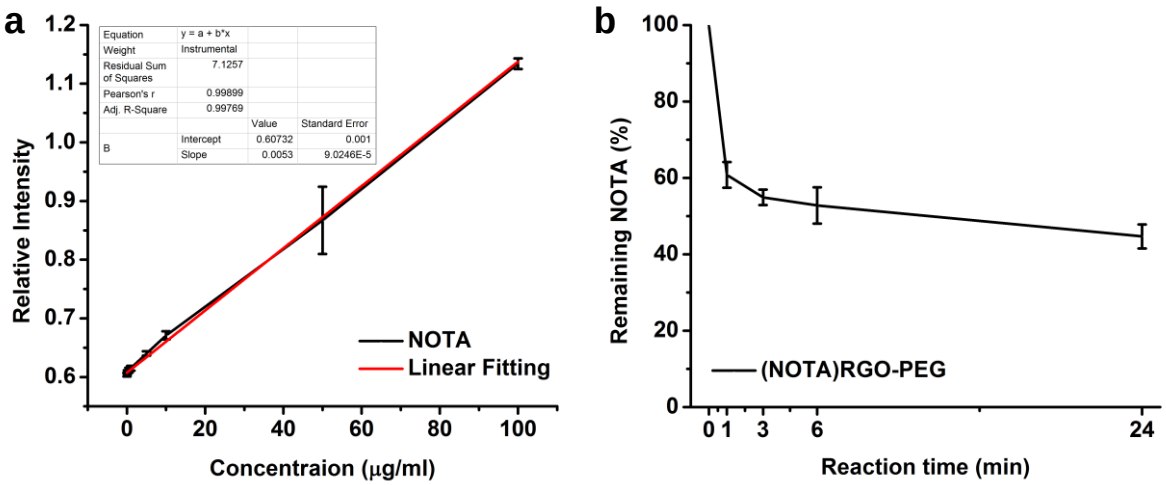

Figure S10. (**a**) Standard curve of UV absorbance at 280 nm based on concentration of NOTA. (**b**) NOTA release profile of (NOTA)RGO-PEG in PBS at room temperature.

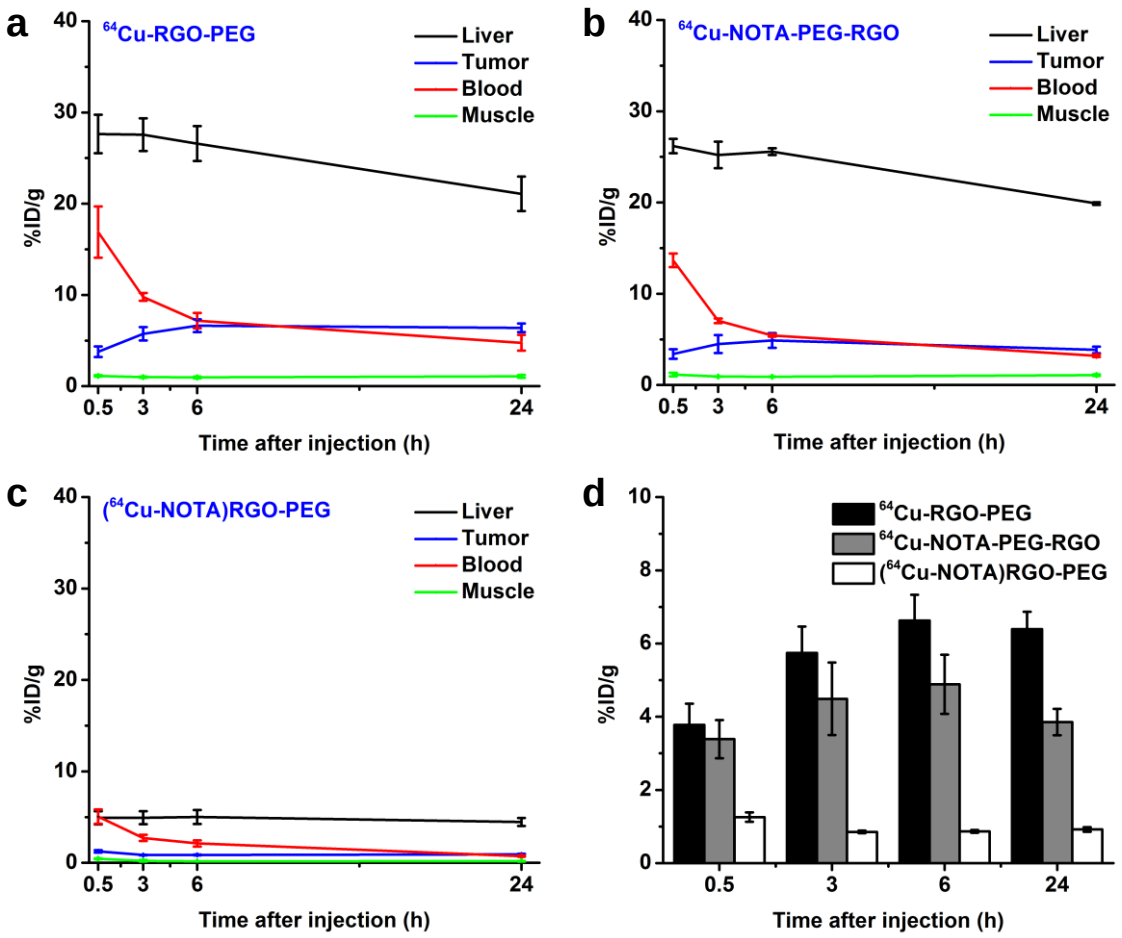

Figure S11. Quantitative analysis of the PET data. Time activity curves of the liver, 4T1 tumor, blood, and muscle upon intravenous injection of ^{64}Cu-RGO-PEG (**a**), ^{64}Cu-NOTA-PEG-RGO (**b**) and (^{64}Cu-NOTA)RGO-PEG (**c**) and comparison of their tumor uptake at different time points (**d**) based on region-of-interest (ROI) analysis.

Table S1. Comparison of the labeling yields of RGO-PEG and GO-PEG at different concentrations and temperatures.

	Concenrations	Labeling yields at different time points (%; RGO-PEG / GO-PEG)				
	(mg/ml)	1 min	15 min	30 min	45 min	60 min
37 ºC	0.05	11.1±1.9 / 4.4±3.3	26.9±3.9 / 5.3±3.3	31.6±3.9 / 5.7±3.6	34.8±4.7 / 6.3±3.7	40.1±4.3 / 6.8±4.0
	0.2	11.4±0.1 / 7.1±0.8	36.7±0.2 / 8.2±0.4	42.0±0.2 / 8.7±0.1	44.9±0.8 / 9.1±0.1	48.0±0.2 / 9.6±0.1
	0.5	22.3±0.1 / 4.1±0.8	41.7±1.3 / 7.3±0.1	47.6±0.6 / 8.4±0.2	50.3±0.4 / 10.1±0.2	58.0±0.1 / 12.8±0.2
75 ºC	0.05	15.0±1.0 / 7.5±1.0	41.1±1.9 / 9.0±1.6	42.9±2.7 / 9.4±1.7	45.1±1.8 / 9.5±1.6	46.0±2.0 / 10.6±1.2
	0.2	18.6±1.1 / 10.6±1.2	62.2±1.1 / 16.1±1.2	69.3±1.9 / 18.2±1.2	72.6±1.8 / 19.3±1.1	76.2±2.1 / 20.8±2.0
	0.5	22.8±2.8 / 13.5±1.5	62.2±1.8 / 15.3±1.3	68.9±2.0 / 15.4±1.6	75.1±1.3 / 15.0±1.2	75.5±1.7 / 15.5±0.8

Table S2. Comparison of the labeling yields with RGO-PEG (37 ºC and 75 ºC), NOTA-PEG-RGO and (NOTA)RGO-PEG (37 ºC) at a concentration of 0.2 mg/ml.

	Labeling yields at different time points (%)				
	1 min	15 min	30 min	45 min	60 min
RGO-PEG (37 ºC)	11.4±0.1	36.7±0.2	42.0±0.2	44.9±0.8	48.0±0.2
RGO-PEG (75 ºC)	18.6±1.1	62.2±1.1	69.3±1.9	72.6±1.8	76.2±2.1
NOTA-PEG-RGO	90.0±0.5	93.1±0.3	93.1±0.5	92.8±0.9	93.1±1.1
(NOTA)RGO-PEG	87.9±1.8	90.7±0.6	91.2±0.6	91.8±0.9	92.1±0.6

Table S3. Comparison of quantitative PET data of chelator-free labeled ^{64}Cu-RGO-PEG, chelator-based labeled ^{64}Cu-NOTA-PEG-RGO and chelator-loaded (^{64}Cu-NOTA)RGO-PEG in 4T1 tumor-bearing mice at different time points after injection.

		Uptake in different tissues at different time points p.i. (%ID/g)			
		0.5 h	3 h	6 h	24 h
^{64}Cu-RGO-PEG (Chelator-free)	Liver	27.6±2.1	27.6±1.8	26.6±1.9	21.1±1.9
	Tumor	3.8±0.6	5.7±0.7	6.6±0.7	6.4±0.5
	Blood	16.9±2.8	9.8±0.4	7.2±0.8	4.8±0.9
	Muscle	1.1±0.1	1.0±0.1	1.0±0.1	1.1±0.1
^{64}Cu-NOTA-PEG-RGO (Chelator-based)	Liver	26.2±0.8	25.2±1.4	25.6±0.4	19.9±0.1
	Tumor	3.4±0.5	4.5±1.0	4.9±0.8	3.9±0.4
	Blood	13.7±0.7	7.0±0.2	5.4±0.1	3.2±0.1
	Muscle	1.1±0.2	0.9±0.1	0.9±0.1	1.1±0.1
(^{64}Cu-NOTA)RGO-PEG (Chelator-loaded)	Liver	4.9±0.7	4.9±0.7	5.0±0.8	4.5±0.4
	Tumor	1.3±0.1	0.9±0.1	0.9±0.1	0.9±0.1
	Blood	5.1±0.8	2.7±0.3	2.1±0.3	0.7±0.1
	Muscle	0.5±0.1	0.2±0.1	0.2±0.1	0.2±0.1

Table S4. Comparison of ex vivo biodistribution with chelator-free labeled ^{64}Cu-RGO-PEG, chelator-based labeled ^{64}Cu-NOTA-PEG-RGO and chelator-loaded (^{64}Cu-NOTA)RGO-PEG at 24 h p.i.

Tissue	^{64}Cu-RGO-PEG (Chelator-free)	^{64}Cu-NOTA-PEG-RGO (Chelator-based)	(^{64}Cu-NOTA)RGO-PEG (Chelator-loaded)
Tumor	5.4±0.9	3.6±0.1	0.7±0.2
Blood	3.5±1.1	2.5±1.1	0.7±0.2
Skin	2.4±1.1	1.3±0.1	0.2±0.1
Muscle	0.6±0.2	0.7±0.2	0.1±0.1
Bone	1.2±0.4	1.2±0.1	0.3±0.1
Heart	5.1±0.4	4.4±0.2	0.6±0.1
Lung	5.9±1.8	7.2±0.1	0.8±0.1
Liver	22.1±4.2	21.7±1.8	5.0±1.3
Kidney	7.3±2.9	7.2±1.1	2.0±0.3
Spleen	11.9±2.8	10.3±1.2	5.6±0.8
Pancreas	1.5±0.2	3.9±1.6	0.2±0.1
Stomach	3.3±1.7	2.9±0.9	0.3±0.1
Intestine	4.5±0.9	4.0±0.6	0.6±0.1
Tail	3.2±0.9	2.5±0.2	0.8±0.1
Brain	0.5±0.1	0.5±0.1	0.1±0.1